Energy Spatial Distribution of Structure Noise Radiated from U-beam Slabs

Li Zhou, Tianqi Zhang, and Yanyun Luo

Abstract At present, the application of U-beams in urban rail transit is gradually increasing, but researches about the bridge structural noise are still insufficient. This article took U-type girder as the research object and studied the structural noise distribution on the basis of energies in different frequency band. Firstly, the dynamic response of the bridge under vehicle load was acquired with the combination of finite element simulation method and field test. Secondly, the structure-acoustic coupling finite element-infinite element model of the U-beam was established, and noise fields of the whole U-beam, the floor and the wing slabs were calculated respectively. By calculating the energies contribution of the sound field point in different frequency bands, the spatial distribution of the radiation noise of the floor and the wing slab in the above frequency bands were obtained. The results show that in the frequency range of 20–200 Hz and the main frequency band (40– 63 Hz), the floor plays a major role in most areas of the whole noise field, and the main influence domain of wing slabs is located in the sector area around wing slabs. In the frequency range of 100–160 Hz, the floor mainly contributes to the acoustic energy of the sector region above and below the U-beam.

Keywords Urban Rail Transit U-Beam · Structure-Borne Noise · Energy Contribution of Slabs

1 Introduction

During the operation of urban rail transit elevated lines, the bridge structure noise generated by vehicle moving mainly concentrated in the low frequency bands [1, 2]. Characteristics of the noise are easy diffraction, long propagation and slow attenuation. Accordingly, the life and work of surrounding residents are affected [3]. Box girder is the most widely used in urban rail transit, and related bridge structure noise

L. Zhou (✉) · T. Zhang · Y. Luo
Institute of Rail Transit, Tongji University, Shanghai, China
e-mail: Li.Z.TJU@hotmail.com; zhouli201007@163.com

has received much researches. For the U-beam, which is very different from the box girder, the research on the U-beam radiation structure noise is insufficient as its application is gradually increasing.

Most existing researches on the structure noise radiated from U-beam mainly focuse on the spectral characteristics and propagation laws, and have made some achievements. Xiaodong Song, et al. [4–6] took the concrete U-beam as the research object, calculated the bridge noise when the train passed by using the 2.5-D acoustic infinite element model, and studied its spectral characteristics and spatial distribution law. Linya Liu et al. [7–9] took the 30 m simply supported U type bridge as the research object, calculated and analyzed the structural noise radiated by the U-beam with the combination of finite element method and acoustic transfer vector method. Jianglong Han [10] used the combining method of vibration power flow, 2-D acoustic simulation and the principle of vibration power equivalence to obtain the radiated sound pressure of the rails and U type bridge. Combined with the field measured noise data of a U-beam, the noise distribution characteristics were analyzed. Minjie Gu and Liu [11] adopted the power flow method to calculate the vibration responses of rails and bridges under vehicle loads. Through the acoustic finite element infinite element method, the generation and propagation of bridge structure noise were analyzed, and the differences in vibration and radiated noise between U-shaped beams and box girder were compared. Jianglong Han et al. [12] used the modal superposition method to calculate the dynamic responses of the vehicle-rail-bridge coupling system. Combined with the modal acoustic transfer vector method, the structural noise of the bridge is calculated. Wu and Liu [13] compared the noise radiation of U beam and box girder, and found that the radiated sound power in the low frequency band of box girder is smaller than that of U beam when the roughness excitation is same.

Generally, there are two main methods to reduce bridge structure noise. One is to reduce the track stiffness, which can reduce bridge structure noise level by lowering bridge vibration, but it possibly brings negative effects such as wheel rail vibration and noise increase [14–16]. The other is to optimize the geometric section of the bridge. At present, the research on the contribution of each slab of U-beam to the sound field of bridge structure noise and the corresponding spatial distribution is not enough. This work is very necessary for contrapuntally reducing the noise level in sensitive areas. Thus, this paper took the U-beam of rail transit as the research object, used the finite element simulation method to establish the vehicle-track-beam dynamic coupling model and structure noise model. Combined with the U-beam vibration test, the frequency spectrum distribution characteristics of vibration and radiated noise of U-beam under vehicle load were analyzed, and the sound field distribution of U-beam radiated structural noise in the 20–200 Hz frequency band is obtained. By changing the boundary conditions of the U-beam radiation noise model, the sound field distribution of the radiation noise of the floor slab and wing slab were acquired. Accordingly, acoustic energy spatial distributions in different frequency bands of different slabs were analyzed.

Fig. 1 Finite element model
of vehicle-track-bridge
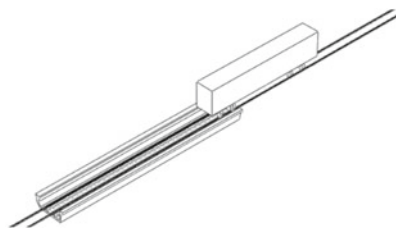
## 2 Dynamic Response Characteristics of U-beam Under Vehicle Load

2.1 Vehicle-Track-U-Beam Finite Element Model

As shown in Fig. 1, the vehicle-track-U-beam dynamic coupling model is established in ABAQUS finite element software. The vehicle body and bogies are simplified as rigid bodies, and the motions of nodding, floating, shaking, and rolling are considered. Wheelsets, rails, track slabs and the bridge are all simulated by C3D8R element. The fastener and bridge supporters are represented by multi-body connection element "cartesian". The vertical stiffness of the fastener is 5×10^7 N/m, and the damping is 5000 N/(m/s). The vertical stiffness of the bridge supporter is 1.26×10^9 N/m. The contact relationship between wheel and rail is defined with surface-surface contact method, and the corresponding normal contact law satisfies Hertz's nonlinear theory [17]. The American track irregularity spectrum is selected as the system excitation, and spatial samples of irregularities (as shown in Fig. 2) obtained from the transformation of the irregularity spectrum by the trigonometric series method [18] are imported to the rail surface. Figure 3 and Fig. 4 show the vibration frequency response results of the U-beam floor slab and wing slab under vehicle load respectively. The main frequency band of floor slab vibration is 40–70 Hz. Besides, there are local peaks in the frequency band of 100–140 Hz. The frequency distribution characteristics of wing slab vibration are basically consistent with that of the floor slab, but the vibration amplitude in the main frequency band of 40–70 Hz is smaller than that of the floor slab.

2.2 Field Test

The U-beam of ordinary monolithic track bed in the actual operation line of urban rail transit is selected as the test section. As shown in Fig. 5, vibration observation points are arranged at the midpoint of the floor slab in the middle of the bridge span, and a vibration measuring point is mounted on the rail bottom as the signal trigger. It is worth mentioning that, considering the complex noise environment (including not only the bridge structure noise, but also the wheel-rail radiated noise, collector noise,

Fig. 2 Level track
irregularity of track
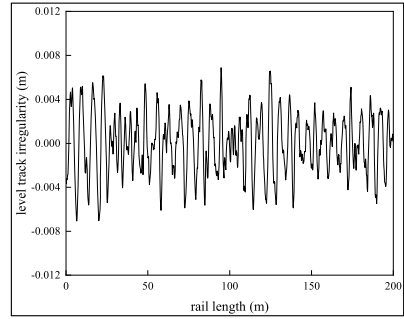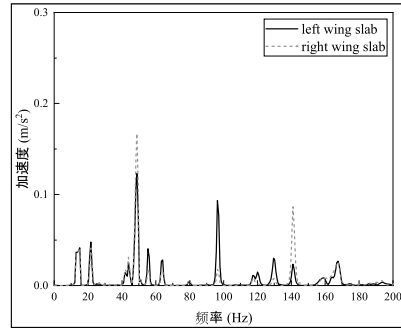

Fig. 3 Vibration
acceleration of floor
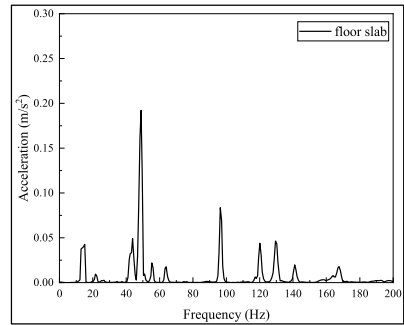
etc.,) around the U-beam during the train passing, this paper did not arrange noise measuring points in the test. Figure 6 shows the vibration octave curve of the U-beam floor slab collected from the test. Obviously, within 200 Hz, the main frequency band of the U-beam floor slab vibration is 40–80 Hz, and the sub main frequency band distributed in the 100–160 Hz frequency band. At the same time, the vibration octave curve of U-beam floor slab obtained by simulation is also drawn in Fig. 6. It is found that the distribution of the main frequency band of the simulation results is slightly different from that of the measured results, and the secondary main frequency band is basically consistent. It can be considered that the finite element simulation model can represent the frequency spectrum characteristics of U-beam vibration under the train load.

3 Spatial Distribution of Radiation Noise of U-beam

The relationship between the vibration and the radiated structural noise of the bridge meets weak coupling law. In another word, slabs vibration has a direct impact on the radiated structural noise, while the effect of the structural noise on the slab vibration can be ignored. Therefore, the finite-infinite element model of the U-beam structural noise shown as Fig. 7 is built in ABAQUS finite element software. The

**Fig. 4** Vibration acceleration of wing slab

Fig. 5 Layout of measuring points for vibration test (unit: mm)
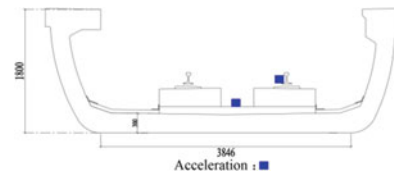
time-domain vibration responses of bridge panels obtained in Section I are applied as the excitation source of the acoustic model to the acoustic-structure coupling interface. In the acoustic model, AC3D8R element is used to simulate air medium, and the corresponding density and bulk modulus of elasticity are 1.2 kg/m^3 and 1.39 $\times$ 10^5 Pa respectively. In order to ensure the calculation accuracy, the maximum element size shall not exceed 1/6 of the wavelength corresponding to the upper limit of the analysis frequency [19]. In this article, the size of elements is around 0.1 m. Furthermore, to avoid the influence of reflected waves generated by the outer boundary, a layer of infinite elements is applied to the outer boundary, and the normal direction of the elements is from the inside to the outside. As in Fig. 8, the midspan section of U-beam is 20 $\times$ 14.8 m range is used as the sound field observation area, and a total of 81 acoustic fields points in 9 rows and 9 columns are selected as the observation points.

Fig. 6 Comparison between measurement and simulation of floor vibration
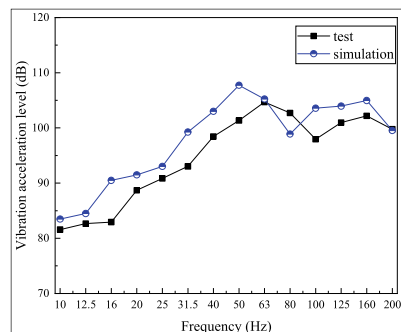
Fig. 7 Finite
element-infinite element
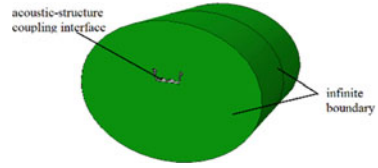model of bridge
structure-borne noise

Figure 9 shows the near-field structure noise spectrum results (20–250 Hz) of the floor slab and two wing slabs obtained by simulation. It can be found that the near-field noise spectrum distribution characteristics of all panels are basically consistent. The main frequency band concentrates in the range of 40–63 Hz, and the secondary frequency band is from100 to160 Hz. The frequency distribution characteristics are basically consistent with the calculated slab vibration spectrum. The difference is that the near-field structure noise in the main frequency band of the floor slab is greater than that of the wing plates. Figure 10 shows the sound pressure level nephogram (20–250 Hz) of the mid span section of the U-beam. This nephogram is not the acoustic field distribution at a certain time during vehicle operation, but the sound field distribution result obtained by linear interpolation method after calculating the total sound pressure level of each sound field observation point during the whole process. The cloud chart mainly displays the overall distribution of the noise of the U-beam structure during the whole process of the train passing. Obviously, the upper and lower regions of the floor slab (corresponding plane coordinate position is −2.5–2.5 m in the horizontal axis and 9–10.8 m in the vertical axis) are noise "hot spots". The noise sound pressure level within the range of 40–80° outside the wing slabs on both sides is relatively small. Within the space region below the U-beam floor slab, the sound pressure level decreases gradually with the increasing distance from the beam.

Fig. 8 Output point of
bridge radiated noise field
(unit: m)
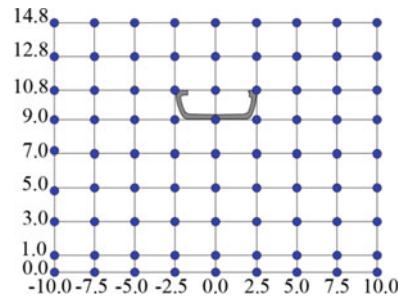
Fig. 9 Near-field noise spectrum of slabs
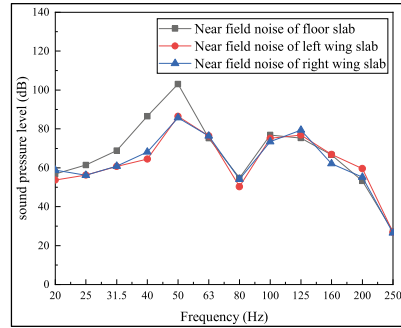
4 Energy Spatial Distribution of Noise Radiated From Each Panel

On the basis of the built U-beam structure-noise model, structure noise respectively radiated from the floor slab and wing slabs can obtained by changing the boundary conditions loaded by vibration excitation. Specifically, by selecting the floor slab and wing slabs as the vibration response mapping area separately, the U-beam floor slab radiation noise model and the wing slab radiation noise model can be built, and the sound pressure level of the radiation noise field caused by the floor slab and wing slabs are respectively calculated.

The corresponding cloud diagrams of the total sound pressure level (20–250 Hz) of during the whole process of vehicle passing are drawn as Fig. 11 and Fig. 12. The sound field distribution of the floor slab is close to the distribution characteristics of the whole U-beam, and there are also noise "hot spots" in the upper and lower region of the floor slab. Due to the shielding effects of two wing slabs, the sound pressure level of the noise in the sector area near two wing slabs is low. The sound field distribution of the wing slab is obviously different. The "hot spots" of the noise are mainly distributed in the fan-shaped area formed by taking the wing slabs on both sides as the center, and center angle is about 160°. With the increase of the distance from the wing slab, the sound pressure level of the field points gradually decreases. At the same time, in the sector area with the vertical line of the floor slab as the axis, the sound pressure level of the field point is smaller and gradually decreases with the increase of the vertical distance from the wing slab.

From the perspective of sound energy, the contribution of panel radiated noise is defined as the ratio of the sound energy of panel radiated sound field points to that radiated from U-beam in unit time. The sound energy per unit area passing through the direction perpendicular to the propagation direction in unit time is sound intensity I, and I is proportional to the square of sound pressure P, therefore, the contribution of panel radiated noise η can be calculated according to formula (1):

$$\eta = \frac{I_{\text{slab}}}{I_{\text{U - beam}}} = \frac{P^2_{\text{slab}}}{P^2_{\text{U - beam}}} \tag{1}$$

Besides,

$$L_p = 10\log_{10}(\frac{P}{P_0})^2 \tag{2}$$

where, L_p is sound pressure level, and P_0 is the reference value

The energy contribution spatial distribution of the floor slab and the wing slab can be obtained through the formula (1) and (2) on the basis of the obtained field point sound pressure level values of noise radiated from the U-beam, floor slab and the wing slab. It is worth noting that the adopted calculation method of panel radiated noise contribution does not take the phase factor of noise radiated by different panels into account, so the total contribution of panel radiated noise maybe exceed 100%. However, the calculation method of this contribution can reflect the contribution of each panel to the total structure noise field from the trend.

Energy contribution nephograms of the floor slab and wing slab are shown as Fig. 13 and Fig. 14 respectively. It can be seen that in the frequency range of 20–ral noise energy in the sector areas with 40–80° extension of both wing slabs are mainly contributed by the wing slab vibration, while the structural noise radiated by the floor slab has a weak influence in this area. Figure 15 and Fig. 16 respectively shows the contribution of the radiated noise from the floor slab and wing slabs on both sides in the main frequency band (40–63 Hz). The distribution tendency of the cloud chart is basically the same as that of panels in the 20–200 Hz frequency band. The main contribution areas of the floor slab are the upper sector area of the U-beam and the sound field below the U-beam bottom plate, and the wing slabs contribute most of the energy of the sound field in the sector area near two wing slabs.

Figure 17 and Fig. 18 respectively shows the radiated noise energy contributions of the floor slab and wing slabs in the sub dominant frequency band (100–160 Hz). It can be seen that in this frequency band, the main contribution area of the floor slab is the upper sector area of the U-beam and the sector area below, while the energy contributions in other areas of the sound field are significantly reduced. Spatial areas with more than 50% contribution of the radiated noise from the wing slabs increased significantly. Main contribution areas distributed in the sector area with the U-beam

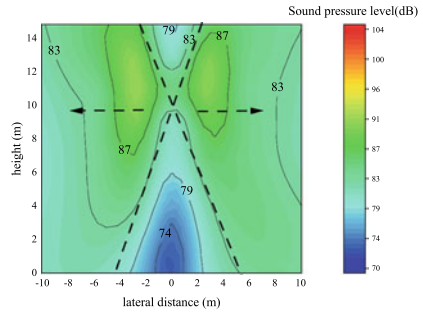**Fig. 10** Nephogram of U-beam structure-borne noise field
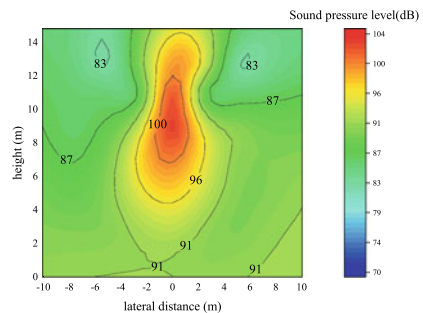
**Fig. 11** Nephogram of noise radiated by floor
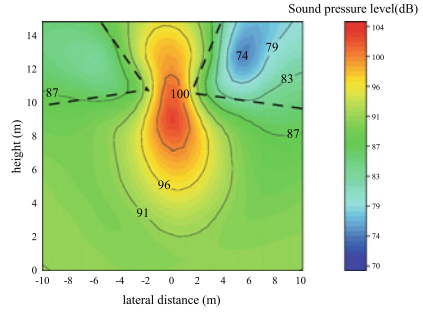
**Fig. 12** Nephogram of noise radiated by wing slabs

as the center, the center line parallel to the bottom plate, and the center angle of about 160°.

In general, in the 20–200 Hz frequency band and the main frequency band of U-beam structure noise, the radiated noise from the floor slab contributes most energies of the whole bridge structure noise field, especially the sector area above the floor slab and the whole field area below the U-beam. The radiated noise from the wing slabs is the main source of the sound field energy of the sector area diagonally above the wing plates of the U-beam. In the sub dominant frequency band (100–160 Hz) of the structural noise, the wing slab contributes most energies of the acoustic field of
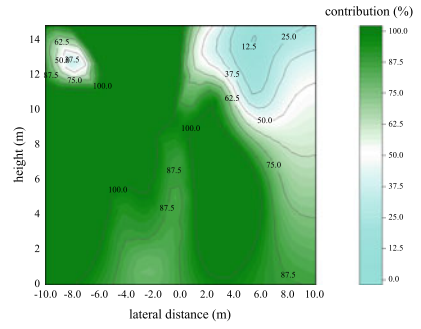
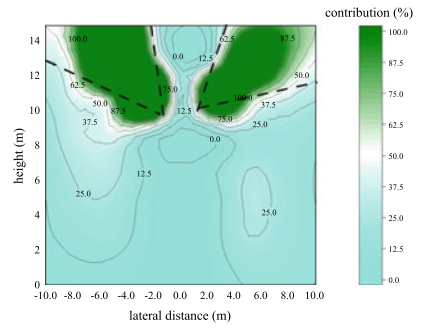**Fig. 13** Spatial distribution nephogram of floor contribution (20–200 Hz)
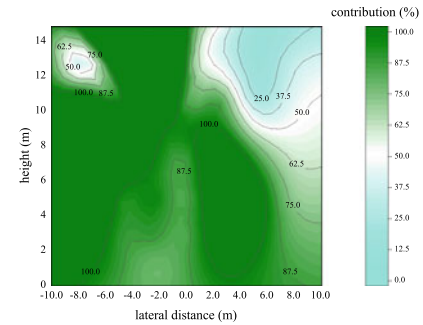
Fig. 14 Spatial distribution nephogram of wing slabs contribution (20–200 Hz)
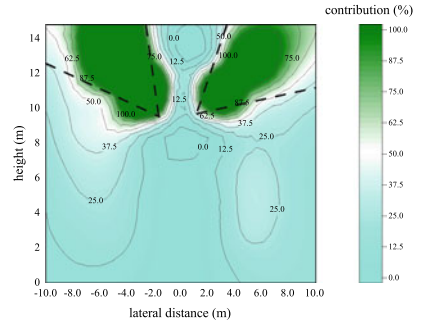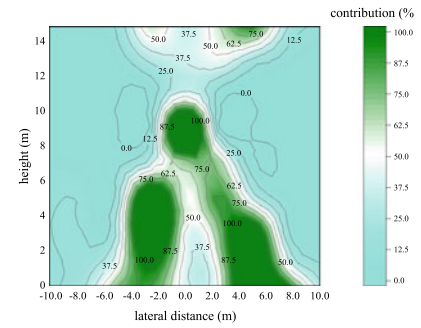

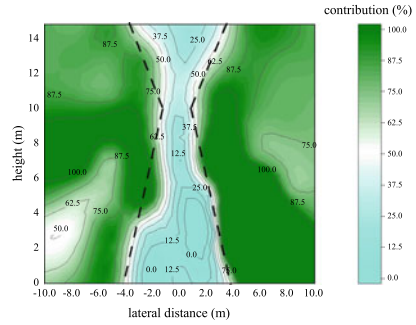**Fig. 15** Spatial distribution nephogram of floor contribution (40–63 Hz)

Fig. 16 Spatial distribution nephogram of wing slabs contribution (40–63 Hz)

Fig. 17 Spatial distribution nephogram of floor contribution (100–160 Hz)

Fig. 18 Spatial distribution nephogram of wing slabs contribution (100–160 Hz)

the bridge structure noise, and the main influenced area by the floor slab is located in the sector area directly above and below the U-beam.

5 Conclusion

In this paper, the urban rail transit U-beam is taken as the research object. The vehicle-track-bridge dynamic coupling model and acoustic-structure coupling model are established in the finite element software. Combined with the test data, the respective radiated noise fields of the floor slab and wing slabs are calculated and analyzed. By introducing the contribution calculation factor, the energy contribution distribution of the floor slab and wing slabs in different frequency bands is acquired. Obtained conclusions are as follows:

(1) In the frequency band of 20–200 Hz, the radiated noise from the U-beam floor contributes most energies of the whole bridge structure noise, and the main influence areas are located below the U-beam floor and directly above the U-beam floor. The main contributed region of the structural noise radiated by the wing slabs vibration is the sector area of 40–80° extension of the wing slabs. The structural noise radiated by the bottom plate has a weaker influence on the sound field of this area.

(2) In the main frequency band (40–63 Hz) of the U-beam structural noise, the energy contribution distribution trend of the floor slab and wing slabs are basically the same as that of the 20–200 Hz frequency band. In details, the floor slab mainly affects the sound pressure level of the sector area directly above the U-beam and that of the lower sector area, and two wing slabs affect the sound field size of the sector area diagonally above the U-beam.

(3) In the sub dominant frequency band (100–160 Hz) of the U-beam structural noise, the floor slab mainly contributes to the sound energy of the sector section directly above and below the U-beam, and the contribution area is greatly

reduced compared with that of main frequency band. The area where the contribution amount of the radiated noise of the wing slabs exceeds 50% is significantly increased. The region is mainly distributed in the sector area with the U-beam as the center, the center line parallel to the bottom plate, and the center angle about 160°.

References

1. Li XZ, Yang DW, Zheng J, et al (2018) Review on vibration and noise reduction of rail transit bridges. China J Highway Transp 31(07):55−75+136
2. He W, H Kewen, Zou C, et al (2021) Experimental noise and vibration characteristics of elevated urban rail transit considering the effect of track structures and noise barriers. Environ Sci Pollut Res 21(03):1–19
3. Liu DY, Wang LZ, Li X et al (2019) Psychoacoustic evaluation index of near-field environmental noise in an intercity railway. Railway Stand Des 63(03):169–174
4. Song XD, Wu DJ, Li Q (2015) A 2.5-dimensional infinite element based method for the prediction of structure-borne low-frequency noise from concrete transit bridges. J Vibrat Eng 28(06):929–936
5. Song XD, Li Q, Wu DJ (2018) Prediction of low-to-medium frequency structure-borne noise radiated from rail transit concrete bridges. J China Railway Soc 40(03):126–131
6. Song XD, Li Q (2019) Numerical study on vibration and noise reduction of rail transit concrete U-shaped bridges. J Southe Univ (Natural Science Edition). 49(03):460–466
7. Liu LY, Qin JL, Lei XY, et al (2018) Low frequency noise of a trough girder structure based on acoustic transfer vector method. J Vibrat Shock 37(19):132–138+152
8. Liu LY, Qin JL, Lei XY, et al (2018) A study on optimization of the structure-borne noise from a trough girder based on response surface methodology. J Vibrat Shock 37(20):56–60+80
9. Liu LY, Qin JL, Liu QM et al (2018) Prediction and optimization of structure-borne low-frequency noise from a rail transit trough girder. J China Railway Soc 40(08):107–115
10. Han JL, Li Q, Gu MJ (2022) Influence investigation of the rail-cum-road viaduct on noise spatial distribution from rail transit traffic. J Vibrat Eng 35:188–195
11. Gu MJ, Li WQ, Li Q (2019) Influence of section types on noise from elevated rail transit lines. J Southw Jiaotong Univ 54(04):715–723
12. Han JL, Wu DJ, Li Q (2013) Calculation and analysis of structure-borne noise from urban rail transit trough girders. Eng Mech 30(02):190–195+202
13. Wu TX, Liu JH (2012) Sound emission comparisons between the box-section and U-section concrete viaducts for elevated railway. Noise Control Eng J 60(4):450–457
14. Sheng X, Zhao CY, Wang P, et al (2018) Effects of fastener stiffness of monolithic bed track on vertical rail sound power characteristics. J Cent South Univ (Science and Technology) 53(05):928–936+1094
15. Zhang X, Su B, Li XZ (2015) Effects of fastener stiffness and damping on structure-borne noise of railway box-girders. J Vibrat Shock 34(15):150–155
16. Cui XL, Chen GX, Yang HG (2017) Influence of wheelset structure and fastener stiffness on rail corrugation. J Cent South Univ (Science and Technology) 52(01):112–117
17. Zhu ZH, Wang LD, Gong W et al (2017) Comparative analysis of several types of vertical wheel/rail relationship and construction of an improved iteration model for train-track-bridge system. J Cent South Univ (Science and Technology) 48(06):1585–1593
18. Chen CJ, Li HC (2006) Track irregularity simulation in frequency domain sampling. J China Railway Soc 03:38–42
19. Miao XH, Qian DJ, Yao XL et al (2009) Sound radiation of underwater structure based on coupled acoustic-structural analysis with ABAQUS. J Ship Mech 13(02):319–324